Relationship between the Structural Conformation of Monoclonal Antibody Layers and Antigen Binding Capacity

Hai Xu

Centre for Bioengineering and Biotechnology, China University of Petroleum (East China), 66 Changjing West Road, Qingdao Economic Development Zone, Qingdao 266555, China

Xiubo Zhao and Jian R. Lu*

Biological Physics Group, School of Physics and Astronomy, University of Manchester, Sackville Street Building, Sackville Street, Manchester M60 1QD, United Kingdom

David E. Williams

Department of Chemistry, University of Auckland, Private Bag 92019, Auckland 1142, New Zealand

Received March 14, 2007; Revised Manuscript Received May 23, 2007

Neutron reflection has been used to determine the pH-dependent structural conformation of monoclonal antibody layers adsorbed at the hydrophilic silicon oxide/solution interface, within the pH range 4−8, over which the silicon oxide surface carried weak negative charges and the net charge on the antibody reversed. The depth resolution achieved, by use of D_2O as solvent to enhance the neutron contrast of the adsorbed antibody layer, was around 2−3 Å. The results have been correlated with the ellipsometric measurement of antigen binding capacity (AgBC). The antibody was a mouse monoclonal anti-hCG (human chorionic gonadotropin) directed against the β subunit of hCG, with molecular weight of 150 000 and isoelectric point around pH 6.0. At pH 4, the adsorbed antibody could be described as a single layer 40 Å thick, consistent with an almost perfect flat-on orientation with all three fragments (Fc, Fab) lying flat on the surface. With increasing pH, the antibody layer swelled (65 Å at pH 6, 75 Å at pH 8) and could be described as three sublayers of different protein density, consistent with some twisting of molecules so that some fragments became more loosely attached to the surface. At pH 8, the repulsive interaction between protein and surface was reflected in a significantly decreased total adsorbed amount. The dominant effect acting to increase AgBC was decreased surface packing density. The effect of the conformational changes revealed at different pH was less important. The results have shown that within the flat-on orientation adopted by the adsorbed antibody, steric hindrance is the main constraint on binding, restricting the access of the antigen to active sites within the antibody layer.

Introduction

Antibodies have been widely employed in various biological and biotechnological applications including immunoassay, biosensor and bioseparation. In these applications, antibodies are immobilized on a solid support surface and used to bind antigens present in fluids. The immobilization can be achieved by either physical adsorption or chemical binding. The former is more widely used because of its simplicity and cost effectiveness. However, surface immobilization causes a significant loss of antigen binding capacity (AgBC) of the antibody.[1−5] Each antibody is a Y-shaped molecule composed of one Fc and two Fab fragments with a molecular weight of some 150 000. Each Fab has a binding site so the theoretical maximum AgBC is equal to 2. Nonetheless, for most currently used immunoassays AgBC is around 0.1 and could be even lower. It is thus crucial to understand the factors affecting AgBC.

It has been widely thought that reduction in AgBC is primarily caused by inappropriate orientation and structural deformation of antibody molecules upon adsorption onto solid surfaces.[6−11] Antibody adsorption onto solid surface has been extensively investigated by techniques including fluorescence,[8,12] reflectometry,[10] calorimetry,[13] surface plasmon resonance (SPR),[11,14−15] ellipsometry,[9,16−17] quartz crystal microbalance (QCM),[18] and Fourier transform infrared spectroscopy attenuated total reflectance (FTIR-ATR).[19] Although these techniques have unraveled useful information about the effect of surface chemistry on the adsorbed amount (surface coverage) and bioactivity, few of them have the right structural resolution to unravel the in situ conformational orientation and distinguish one orientation from another. Because protein layers are ultrathin, heterogeneous, and heavily mixed with water, the change in refractive index across the interface arising from protein adsorption is small. Techniques such as optical reflectometry, surface plasmon resonance (SPR), and ellipsometry base their measurements on detecting the change of refractive index, and although they are able to provide useful estimates of the adsorbed amount, they have little inherent sensitivity to layer thickness and composition.

Neutron reflection (NR) can alleviate most of these limitations. Its structural sensitivity arises from the short neutron wavelength, typically ranging from 1 to 10 Å. This range of neutron wavelength is comparable to the dimensions of protein molecules, making the method intrinsically more sensitive than optical reflection and SPR. The high structural resolution of NR can be enhanced by exploiting isotopic contrast variation. Neutron scattering varies strongly with H/D isotopic substitution. By measurement of antibody adsorption in D_2O, the thickness

* To whom correspondence should be addressed: phone 44-161-2003926; e-mail j.lu@manchester.ac.uk.

10.1021/bm070297u CCC: $37.00
Published on Web 07/07/2007

and composition of the protein layer can be determined unambiguously. Neutron reflection is able to reveal layer thickness with resolution better than a few angstroms. The advantageous features of NR in the direct characterization of the in situ structural conformations of protein layers adsorbed at the solid/liquid interface have been well demonstrated,[20−32] but it has hardly yet been used to link the structural conformation of antibody to activity in antigen binding.[33]

The antibody used in this work was a mouse monoclonal anti-hCG (human chorionic gonadotropin) directed against the β subunit of hCG. Its isoelectric point (IP) is around pH 6. The overall molecular charge density increases as the pH is shifted away from the IP.[10,34,35] Thus a pH shift will alter the electrostatic interactions within the protein layer. At the same time, the silicon oxide surface above pH 2 carries a small negative charge. According to Iler,[36] the negative charge density shows only a weak variation over the range pH 3−8. Thus the SiO_2 surface is ideal for examining how electrostatic interactions within the antibody layer and between the layer and the surface affect the adsorbed amount and orientation, and to relate the observed changes to changes in AgBC. In the present study we have employed neutron reflection to examine the in situ pH dependence of anti-β-hCG adsorption onto a silica surface under a range of solution pH. Our results have shown that the surface excess of antibody attains its maximum around its IP, similar to the trend observed for other proteins, such as lysozyme and human serum albumin. Importantly, the adsorbed layer primarily adopts a "flat-on" orientation under all pH conditions studied and there is no obvious indication of the "side-on" or "tail-on" orientations that would expose one or two Fab fragments for easy antigen binding. Within the "flat-on" orientation, the detailed structure and composition within the antibody layer does vary with solution pH. However, the antigen binding capacity shows a straightforward relation with the surface adsorbed amount of antibody and rather less influence of the detailed surface conformation, suggesting the dominance of simple steric effects on AgBC.

Neutron Reflection

In a neutron reflection measurement, the reflectivity of neutrons $R(\kappa)$ is measured as a function of the wave vector κ perpendicular to the reflection surface. The relationship between $R(\kappa)$ and the structure of an interfacial layer can be outlined from the following three equations:[37]

$$R(\kappa) = \frac{16\pi^2}{\kappa^2}|\hat{\rho}(\kappa)|^2 \quad (1)$$

$$\hat{\rho}(k) = \int_{-\infty}^{\infty} \exp(-i\kappa z)\rho(z)\, dz \quad (2)$$

and

$$\rho = \sum n_i b_i \quad (3)$$

where $\rho(z)$ is the scattering length density along the surface normal direction (z-direction) and n_i is the number density of ith element with scattering length b_i.

Although neutron reflectivity can in principle be Fourier-transformed into the scattering length density profile, data analysis is more conveniently handled via model fitting based on optical matrix formulas. Briefly, a structural model is assumed, which consists of a series of layers, each with a scattering length density ρ and thickness τ, and the corresponding reflectivity is calculated.[37] The calculated reflectivity is then compared with the measured one, and the structural parameters are subsequently varied in a least-squares iteration until the optimal fit is found.

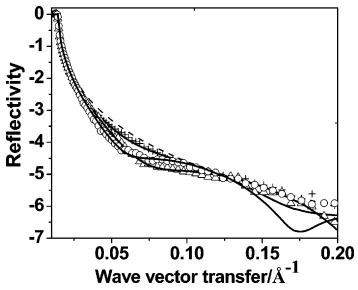

Figure 1. Neutron reflectivity profiles at the silica/D_2O interface at solution pH of 4 (△), 6 (○), and 8 (+). The anti-β-hCG concentration was fixed at 10 mg·L^{-1} and the ionic strength at 20 mM. The reflectivity profile from the bare silica/D_2O interface is also shown for comparison (dashed line). The continuous lines were the best fits calculated from the single uniform layer model with $\tau = 40 \pm 3$ Å and $\Gamma = 2.2 \pm 0.3$/mg·m^{-2} at pH 4; $\tau = 50 \pm 3$ Å and $\Gamma = 2.8 \pm 0.3$/mg·m^{-2} at pH 6; and $\tau = 52 \pm 3$ Å and $\Gamma = 1.3 \pm 0.3$/mg·m^{-2} at pH 8. Other parameters are listed in Table 1.

Results and Discussion

(1) Antibody Adsorption at Different pH. At the beginning of the neutron reflection experiment, we first determined the thickness of the thin native oxide layer present on the silicon surface. D_2O was used to highlight the structure of the oxide layer. The reflectivity obtained at the bare silicon oxide/D_2O interface is shown as the dashed line in Figure 1. The measured reflectivity profile could be fitted to a uniform layer model with a thickness of 14 ± 2 Å and a corresponding scattering length density (ρ) of 3.41×10^{-6} Å^{-2} for the oxide layer. As ρ is the same as that of amorphous silicon oxide, it was assumed that the oxide layer contained no voids or cavities. The good fit to a uniform layer model without the need for incorporating roughness also indicated the smoothness of the oxide layer.

Figure 1 shows the measured reflectivity profiles plotted as a function of wave vector κ at solution pH 4.0, 6.0, and 8.0, with the anti-β-hCG concentration fixed at 10 mg·L^{-1}. With reference to the reflectivity from pure D_2O, anti-β-hCG adsorption altered the shape of the reflectivity curve. The main feature from these reflectivity profiles was the occurrence of a broad interference fringe between 0.05 and 0.1 Å^{-1}. The gradient of the profile in this wave vector range, pH 6 > pH 4 > pH 8, indicates that the adsorbed amount was pH 6 > pH 4 > pH 8. The reflectivity measurements therefore show the occurrence of maximum adsorption at the IP for the antibody. Thus it appears that the dominant influence on the amount adsorbed was electrostatic repulsions within the adsorbed protein layer, rather than the electrostatic attraction to the surface.

To obtain quantitative information about the amount of adsorbed anti-β-hCG, the measured reflectivity profiles at different pH values were fitted by the optical matrix method as already outlined.[37] The fitting was started with the simplest model, of a uniform layer for the adsorbed anti-β-hCG, as it carried the least number of variables. The continuous lines in Figure 1 are the best fits to this model, where it is assumed that the structure of the oxide layer stayed the same as in pure D_2O. The volume fraction (φ_p) and the surface excess (Γ) of

the protein within the layer can be calculated from the following equations:

$$\varphi_p = \frac{\rho - \rho_w}{\rho_p - \rho_w} \quad (4)$$

$$\Gamma = \varphi_p \tau \rho'_p \quad (5)$$

where ρ_p and ρ_w are the corresponding scattering length densities for the antibody and water, ρ'_p is the antibody's mass density, and ρ_w for D_2O is 6.35×10^{-6} Å^{-2}. To calculate the scattering length density of the antibody, we assumed a typical IgG sequence and complete exchange of the labile hydrogens between antibody and D_2O. This was found to be right within a few percent error in surface excess, but uncertainty had no effect on layer thickness.[23−25] The scattering length density of anti-β-hCG in D_2O was calculated to be 3.36×10^{-6} Å^{-2}.[33] IgG has a molecular weight of 150 000, and its molecular volume is around 1.76×10^5 Å^3, producing a mass density of 1.42 g·mL^{-1} for this protein.

The layer thickness and scattering length density obtained from fitting to each of the reflectivity profiles is given in Table 1. Figure 1 shows excellent fit to the reflectivity measured at pH 4.0, indicating that the layer were well represented by a uniform protein distribution along the surface normal direction. At pH 6.0 and 8.0, the uniform layer fits to the measured reflectivity profiles were satisfactory below 0.13 Å^{-1}, but deviations occurred over the high wave vector transfer range. These differences indicate the presence of nonuniform features within a broadly uniform structural distribution. Although the uniform layer model may be inadequate for describing the protein layer structure in these cases, it is sufficiently accurate for determining the adsorbed amount.[38]

It should be noted that, to avoid possible inconsistency caused by time-dependent adsorption, all the NR measurements in this study were made after 30 min adsorption. Time-dependent anti-hCG adsorption onto the silica surface has previously been carried out at 7.5[34] and 10[35] mg·L^{-1} over a wide pH range, and the surface-adsorbed amount reached plateau values within 30 min, consistent with our observation in this part of the study.

Figure 2 compares the surface excesses obtained from neutron reflectivity with results obtained from our previous ellipsometry study[35] and also from the work by Buijs et al.[10,34] under similar surface and solution conditions. In line with the qualitative discussion given above, the data all show a maximum in adsorption around the IP for the antibody (pH 6). The agreement between the different measurements is good at pH 4 and 6 but less so at pH 8. It can also be seen from Figure 2 that the maximal surface excess at pH 6 was 2.77 mg·m^{-2}, close to the theoretical saturation limit derived from typical molecular dimensions of IgG of 3.0 mg·m^{-2} for the "flat-on" monolayer orientation, indicating that the monolayer was well packed. As the pH is moved away from the IP, the net charge density on the antibody rises, so the increased lateral electrostatic repulsion may be the cause for the decreasing surface excess.

As already indicated, the silicon oxide surface is negatively charged and its negative charge density increases slightly when pH increases from 3 to 8.[36] Below pH 6.0, the net charge on the anti-β-hCG would be positive and the protein layer would be electrostatically attracted to the solid surface, but the interaction would be repulsive between the charged protein molecules within the layer. The observed decrease of surface excess below pH 6.0 indicates the significance of the lateral protein−protein repulsion for determining the anti-β-hCG amount adsorbed onto the silicon oxide surface. Above pH 6, when both the protein and the solid surface would be negatively charged, the reduction in the adsorbed amount was greater, interpretable as due to charge repulsion between protein and surface acting in addition to the repulsion within the adsorbed layer. Thus, the pH dependence of anti-β-hCG adsorption onto the oxide surface is determined by the combined electrostatic effect of the lateral protein−protein repulsion and the protein−surface interaction. While the overall surface excess profile is dictated by the lateral electrostatic repulsion, the weakening of protein−surface interaction at high pH has consequential effects on the structural conformation of the antibody, as will be described below.

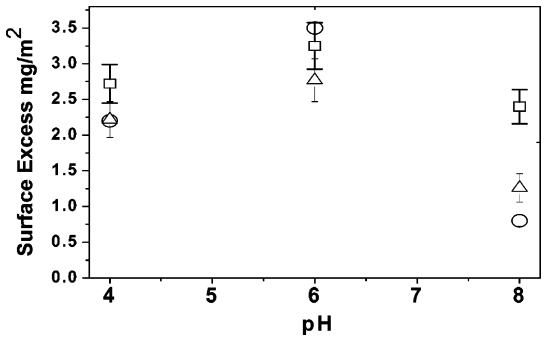

Figure 2. Surface excesses obtained from the NR measurements (△) as a function of solution pH. The protein concentration and the solution ionic strength were fixed as 10 mg·L^{-1} and 20 mM, respectively. For comparison, the surface excesses (□) obtained from the previous ellipsometric measurements by us and those (○) obtained by Buijs et al.[10,34] are also shown.

Table 1. Structural Parameters Obtained from the Single Uniform Layer Model

pH	τ, Å	$(\rho \pm 0.05) \times 10^6$, Å^{-2}	$\varphi \pm 0.02$	$\Gamma \pm 0.3$, mg·m^{-2}
4.0	40 ± 3	5.20	0.39	2.22
6.0	50 ± 3	5.20	0.39	2.77
8.0	52 ± 5	5.85	0.17	1.26

(2) Structural Conformation of Antibody Layers. Neutron reflectivity provides direct information about layer thickness and the extent of water mixing, with a depth resolution of 2−3 Å. This depth resolution for probing interfacial structure at the solid/water interface is presently unavailable from most other techniques. In NR, the measured thickness of the adsorbed protein layer is usually compared with the known dimensions of the protein to determine its conformational orientation and the extent of structural deformation arising from the contact with the solid surface.

As indicated in the foregoing section, a single uniform layer with thickness of 40 Å and scattering length density of 5.2×10^{-6} Å^{-2} was adequate for describing the reflectivity measured at pH 4.0, indicating that the average volume fraction of the adsorbed antibody molecules projected onto the interface normal direction was approximately uniform and that there was no need to have two or more sublayers to account for the nonuniformity. An antibody molecule has approximate dimensions of $142 \times 85 \times 38$ Å^3.[39−41] Because the thickness determined for the antibody layer was close to the short axial length, the result suggests that the antibody adopted a "flat-on" orientation with all three fragments in direct contact with the surface. In order to assess the reliability of the fitted layer thickness, the reflectivity profiles calculated from thicknesses of 30 and 50 Å were also compared with the measured one. In each of the

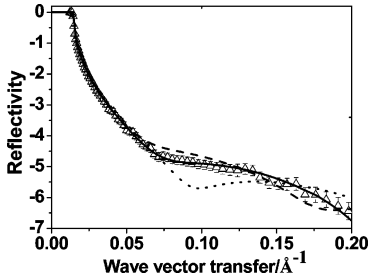

Figure 3. Uniform layer modeling of the reflectivity profile at pH 4.0 in the presence of 10 mg·L^{-1} anti-β-hCG. The continuous line was calculated with a layer thickness of 40 Å and a scattering length density of 5.2 $\times$ 10^{-6} Å^{-2}. The dashed and dotted lines were calculated for layer thicknesses of 30 and 50 Å, respectively.

Table 2. Structural Parameters of Anti-β-hCG Layers[a]

pH	τ, Å	($\rho \pm 0.05$) $\times$ 10^6, Å^{-2}	$\varphi \pm 0.02$	$\Gamma \pm 0.3$, mg·m^{-2}
4.0	$\tau_1 = 40 \pm 3$	$\rho_1 = 5.20$	$\varphi_1 = 0.39$	2.22
6.0	$\tau_1 = 10 \pm 3$	$\rho_1 = 5.60$	$\varphi_1 = 0.25$	2.80
6.0	$\tau_2 = 30 \pm 3$	$\rho_2 = 5.00$	$\varphi_2 = 0.45$	
6.0	$\tau_3 = 25 \pm 5$	$\rho_3 = 5.90$	$\varphi_3 = 0.15$	
8.0	$\tau_1 = 10 \pm 3$	$\rho_1 = 6.10$	$\varphi_1 = 0.08$	1.45
8.0	$\tau_2 = 30 \pm 3$	$\rho_2 = 5.70$	$\varphi_2 = 0.22$	
8.0	$\tau_3 = 35 \pm 5$	$\rho_3 = 6.10$	$\varphi_3 = 0.08$	

[a] Solution pH was at the bulk concentration of 10 mg·L^{-1}. Solution ionic strength was fixed at 20 mM.

calculations the scattering length density for the corresponding layer was adjusted to produce the best fit. The results are given in Figure 3. It can be seen that the fit to the reflectivity profile produced at thickness of 40 Å is significantly better than the other two, indicating the sensitivity of the technique to the adsorbed protein layer thickness. Because the reflectivity is highly sensitive to layer thickness, any obvious deviation away from 40 Å would lead to visible disagreement between the calculated and the measured profiles as shown in Figure 3, suggesting that neither side-on (thickness 85 Å) nor head-on/tail-on (thickness 140 Å) orientations on the silica surface would occur at pH 4.0.

At pH 8, the measured reflectivity profile was best fitted by a three-layer model with total thickness of 75 Å. The model consisted of an inner sublayer (next to the silicon oxide) of 10 Å, a middle sublayer of 30 Å and an outer sublayer of 35 Å, with corresponding protein volume fractions of 0.08, 0.22, and 0.08 (Table 2). The account of the variation in the volume fraction distribution along the interfacial normal direction clearly led to the improvement of the fitting from the best uniform layer model described earlier. An interpretation is that there was some twisting of some of the adsorbed molecules, due to the lateral and interfacial repulsions outlined previously, leading to projections of Fc and Fab fragments somewhat away from the surface. Thus the depletion of antibody fragments within the inner 10 Å sublayer reflected the electrostatic repulsion between the protein layer and the surface, and the outer 30 Å sublayer reflected the fragment distribution associated with the increased lateral repulsion. The main body of the antibody was clearly within the middle sublayer, showing that in spite of a broadened orientation distribution driven by the electrostatic repulsion, the antibody again dominantly adopted a "flat-on" orientation. Any broadening effect such as electrostatic repulsion would make the distribution much broader. This shows that it is unlikely that the adsorbed antibody exhibited side-on or "standing-up" orientation on the surface.

It should be noted that the surface adsorption at pH 4 was greater than at pH 8. This difference may arise from the different

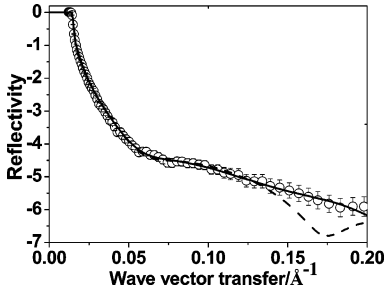

Figure 4. Three-layer model fit to the measured reflectivity at pH 6.0 in the presence of 10 mg·L^{-1} anti-β-hCG. The continuous line was calculated from the parameters given in Table 2. For comparison, the best fit from uniform layer model is also shown (dashed line).

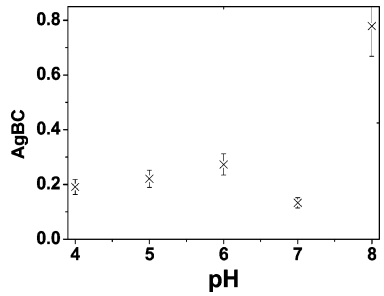

Figure 5. Variation of AgBC with pH. The antibody layer was obtained by incubating in 10 mg·L^{-1} anti-β-hCG solution at an ionic strength of 20 mM. The antigen binding and the antibody preadsorption were performed at the same pH and ionic strength. The experimental detail is in ref 35.

electrostatic repulsions at pH 4 and 8. Note that the antibody molecules are adsorbed entirely "flat-on" at pH 4 with little fragment tilting and twisting, an observation different from the situation at pH 8. The protein−surface electrostatic interaction is attractive at pH 4 but repulsive at pH 8. The attractive force at pH 4 must be strong enough to avoid the presence of the inner depletion sublayer and prevent the fragments from adopting any twisting out of the flat-on orientation.

At pH 6.0, the net charge on the antibody is zero and the overall lateral repulsion would be minimal. It is expected that a uniform protein monolayer would be formed at the interface. This, however, was not the case as is shown in Figure 1 and Figure 4 (dashed line). Instead, a three-layer model consisting of an inner sublayer of 10 Å, a middle sublayer of 30 Å, and an outer sublayer of 25 Å provided the best fit, as depicted in Figure 4. The corresponding protein volume fraction in each sublayer was 0.25, 0.45, and 0.15, reflecting the extent of nonuniformity within the predominantly flat-on orientation at the interface. This model is broadly similar to that obtained at pH 8.0 except for the greater protein volume fraction, within the inner sublayer, consistent with weaker electrostatic repulsion between the protein layer and the oxide surface at pH 6. Differences in local charges on the fragments may cause preferential distributions within the layer and may thus be responsible for causing the inhomogenous distribution. The three-layer model could also be accounted for by a combination of an equal amount of straight flat-on monolayer 40 Å thick and tilted flat-on monolayer of 65 Å thickness, with both orientations adopting a depleted region of 10 Å thick next to the oxide layer arising from local charge effects and steric hindrance.

(3) Efficiency in hCG Binding. Each anti-β-hCG has two Fabs and should be able to bind two hCG molecules, giving maximal AgBC = 2. Figure 5 shows the actual AgBC, measured by spectroscopic ellipsometry, against solution pH. The AgBC

measurement has been described previously.[35] Preadsorption of anti-β-hCG was performed under the same solutions as used for neutron reflection. Briefly, after preadsorption in 10 mg·L^{-1} anti-β-hCG solution, surface rinsing by replacing the antibody solution with phosphate buffer and postcoating with bovine serum albumin (BSA) were carried out, followed by addition of 2 mg/L antigen solution, with the same solution pH and ionic strength during the whole process. It is apparent that between pH 4 and 7 AgBC was almost constant between 0.1 and 0.3. At pH 8, AgBC rose to a very high value of 0.8. We showed above that over the entire pH range the antibody adopted a predominantly flat-on orientation, changing from a well-packed uniform layer of 40 Å at pH 4 to a "diffused" uneven distribution at higher pH. Over the pH range between 4 and 7, the surface excess varied but was in all cases above 2 mg/m^2.[35] In contrast, the surface excess at pH 8 was lower: 1.4 mg/m^2. The reduction in surface excess and the blurring of protein distribution can be linked. It can be concluded that the surface packing density of the antibody was the main factor affecting AgBC.

HCG has molecular weight around 38 000, consisting of two subunits. The two subunits noncovalently associate to form a dimer, with dimensions of 75 Å × 35 Å × 30 Å.[42] Because it is rather large, there should be significant steric hindrance to access of hCG molecules to the binding sites inside the middle and inner sublayers. This would particularly be the case at pH 4, where the whole layer is close-packed, and at pH 6, where the middle sublayer is even more close-packed. Furthermore, our hCG has an isoelectric point around 5.5, close to that for the antibody. Because the outer surface of hCG also carries charged groups, electrostatic interactions may also become important when the solution pH is shifted away from the IP. The AgBC did have a discernible maximum near pH 6, near the IP of both antibody and antigen. However, the relatively small variation in AgBC between pH 4 and 7 suggests that the electrostatic repulsion effects between antibody and antigen are not the most important determinant of AgBC. At pH 8, where the AgBC was markedly increased, the overall layer structure broadly resembled that at pH 6. Electrostatic repulsion effects would be the strongest at pH 8. The high AgBC must therefore be a consequence of the low surface packing density of the antibody. We have recently studied the variation of AgBC with surface excess of the antibody at pH 7 and observed a steady decrease of the AgBC with increasing antibody surface excess.[35] Interestingly, the AgBC at the same surface excess as that observed here at pH 8 was also around 0.8, again implying that other effects such as particular structural conformations or different electrostatic interactions have much less effect on AgBC than the simple variation of surface packing density.

To ascertain the reliability of hCG binding measurements, two control experiments were undertaken. In the first control experiment, hCG binding was measured without any antibody adsorption. The bare silicon oxide surface was preadorbed with 1 mg/mL BSA, followed by the buffer rinsing and equilibration, and then replaced by 2 mg/L hCG solution for its binding measurement. It was found that the BSA adsorbed amount was reproducible at the three pH values, and the amount of hCG bound was close to 0 and 0.03 mg/m^2 at pH 4 and 6 and was 0.15 mg/m^2 at pH 8 The relatively high hCG binding at pH 8 was mainly due to the low BSA adsorption (0.2 mg/m^2 at this pH). The second control experiment was done at pH 8, with the full hCG binding experimental procedure under identical conditions. But instead of anti-β-hCG (at 10 mg/L), human plasma IgG was used. No measurable amount of hCG was detected under all three pHs studied. It can thus be concluded that the hCG binding shown in Figure 5 must arise from specific recognition.

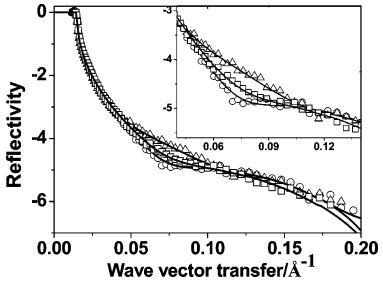

Figure 6. Variation of reflectivity of the adsorbed anti-β-hCG layer with respect to test solution pH. The adsorption was started at pH 4.0 in the presence of 10 mg·L^{-1} anti-β-hCG (○), then the protein solution was replaced with a pH 4.0 buffer (○), followed by a change to a pH 8.0 buffer (△), and finally followed by replacement of pH 8.0 buffer with a new pH 4.0 buffer (□). The continuous lines were the best fits for the parameters given in Table 3. The inset shows variations more clearly by expanding the κ range between 0.05 and 0.15 Å^{-1}.

Table 3. Structural Parameters Obtained from pH Cycling by Use of pH Buffers

pH	τ, Å	$(\rho + 0.05) \times 10^6$, Å^{-2}	$\phi \pm 0.02$	$\Gamma \pm 0.3$, mg·m^{-2}
4.0	$\tau_1 = 40 \pm 3$	$\rho_1 = 5.2$	$\phi_1 = 0.39$	2.14
8.0	$\tau_1 = 10 \pm 3$	$\rho_1 = 6.10$	$\varphi_1 = 0.08$	1.45
8.0	$\tau_2 = 30 \pm 3$	$\rho_2 = 5.70$	$\varphi_2 = 0.22$	
8.0	$\tau_3 = 35 \pm 5$	$\rho_3 = 6.10$	$\varphi_3 = 0.08$	
4.0	$\tau_1 = 40 \pm 3$	$\rho_1 = 5.6$	$\varphi_1 = 0.25$	1.43

Different IP values for hCG have been reported.[43,44] The difference could arise from the different number of N- and O-linked oligosaccharides. Altered IP could affect the pattern of hCG binding between pH 4 and 7.5 as shown in Figure 5, but how the structure and chemical nature of these oligosaccharide side chains affect hCG adsorption and binding needs to be studied.

(4) Tuning Interfacial Structure by Varying pH. Variation of solution pH and antibody concentration is a simple and useful practical means to adjust antibody surface loading and activity in immunoassay devices. Furthermore, in many practical applications of immunoassay, the test solution pH may vary. It is thus useful to examine how pH shift affects the preadsorbed antibody (the adsorbed amount and the antibody layer structure) and the subsequent AgBC.

Figure 6 shows the reflectivity measured at an initial pH 4.0 in the presence of 10 mg·L^{-1} anti-β-hCG. The pH 4 protein solution was then replaced by a pH 4.0 buffer: the reflectivity did not change, showing no desorption at this pH as a consequence of the removal of the protein from the solution. The complete irreversibility may arise from the electrostatic attraction between the protein and the surface. The solution was then changed to a pH 8.0 buffer and finally back to the pH 4.0 buffer. When the buffer pH was increased to 8.0, there was a clear change in the shape of the reflectivity profile. This reflectivity profile was found to be identical to that obtained from direct adsorption from the 10 mg·L^{-1} anti-β-hCG solution onto the fresh silicon oxide surface at pH 8.0, and the corresponding interfacial structure was also well represented by the same three-layer distribution (Tables 3 and 2). Thus, protein had desorbed to a level characteristic of a surface saturated with protein at pH 8, giving a surface structure characteristic of this pH and not of the route used to reach the

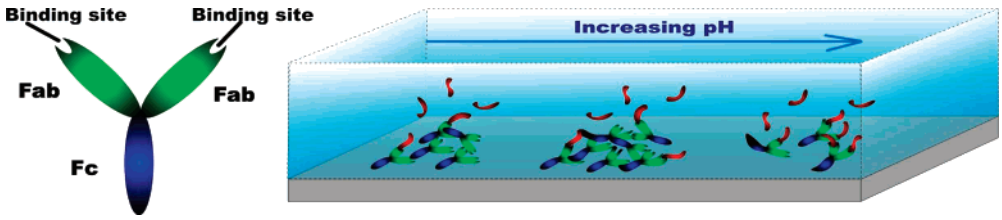

Figure 7. Schematic representation to show the gradual pH-dependent transition of antibody structural conformation and hCG binding. Electrostatic repulsions at higher pH cause the layer to twist and open up. The opening up of the antibody's constituent fragments, within a predominantly "flat-on" orientation, leads to the increase in AgBC. Color coding: Fc is shown in blue, Fab in green, and hCG in red.

particular surface composition. When the pH 8.0 buffer was replaced by pH 4.0 buffer again, the reflectivity was well represented by a 40 Å uniform layer distribution, except that the surface excess had remained almost constant, at 1.45 mg/m^2, the same as that at pH 8, showing no protein desorption during this pH change. The structural parameters obtained from the fitting to the reflectivity profiles during the pH cycle are listed in Table 3. If there were any significant irreversible surface denaturation of the protein, then the layer structure obtained by adsorption and then pH shift ought to be different than that obtained by direct adsorption at the final pH. The conclusion is that there was no significant denaturation of the protein on the surface and that the surface conformation was determined solely by the charges on protein and surface.

The AgBC of the different layers was measured. At the starting point (pH 4.0), AgBC was 0.2 as shown above. When the pH 4.0 buffer was replaced by the pH 8.0 buffer, AgBC was 0.8, which is the same as that obtained from direct adsorption at pH 8, consistent with the observation that the layer structure resulting from the two different preparation routes was the same. When the buffer pH was returned back to pH 4.0, although the surface excess kept constant during this process, the AgBC decreased, but to a value of 0.4, intermediate between that at the pH 4 starting condition and the pH 8 condition. The increase in AgBC from the starting value at pH 4 is directly attributable to the decrease of surface excess. The decrease from the value measured at pH 8 is attributable to the antibody packing down more tightly onto the surface: the conformation changed from a loose three-layer structure with total thickness of 75 Å at pH 8 to a relatively well-packed uniform layer with thickness of 40 Å at pH 4. Above, we discussed the effects of charge changes on the binding and deduced that they were relatively small.

Conclusions

Many current biotechnological developments such as biosensors, immunoassays, and biocatalysis would benefit from a better understanding of how proteins interact with support substrates in the presence of water. Upon adsorption or immobilization, many different factors can contribute to the interaction, resulting in different interfacial structure and composition and different consequences for antigen binding. Strong protein−substrate interaction could lead to structural unfolding and loss of bioactivity. Even under the conditions where interaction is not strong and protein is robust, inappropriate conformational orientation could also reduce bioactivity. Immunoglobulin Gs are an important class of protein molecules. The four polypeptide chains are grouped into two identical Fab segments and one Fc segment, and the whole molecule adopts a Y-shaped conformation. As previously outlined, the hCG binding sites are located on the far ends of the Fab segments. While there is sufficient flexibility between Fab and Fc segments, each segment retains globular stability. This work has aimed at revealing the conformational structure of anti-β-hCG at the hydrophilic silicon oxide/water interface by use of neutron reflection and linking the structural information to hCG binding capacity.

The pH-dependent antibody adsorption and hCG binding is outlined schematically in Figure 7. Our neutron reflectivity measurements showed that over the entire pH range studied the antibody adopted a predominantly flat-on orientation. The major influence on the AgBC was the surface excess of antibody, changes that could be induced by pH-dependent changes in the electrostatic interactions within the protein layer and between protein and surface. Steric hindrance of access of antigen to antibody binding sites within the layer was the major determinant of AgBC. At a fixed surface excess, swelling of the protein layer, caused by charge repulsion from the surface, resulted in an increased AgBC. There was no evidence for the currently accepted paradigm that antigen binding by surface adsorbed antibody requires side-on or tail-on orientations with Fab fragments exposed to the solution side so that antigen molecules can easily access them. In fact, there appears to be a much more subtle interplay of factors, in which the surface packing density of antibody is the most important, that allows antigen access to antibody binding sites with the antibody adsorbed flat-on to the interface.

Experimental Section

Neutron reflectivity measurements were made on the white beam reflectometers CRISP and SURF at the Rutherford−Appleton Laboratory, ISIS, Didcot, U.K., with neutron wavelengths from 1 to 6.5 Å. A silicon ⟨111⟩ block with dimensions of 2.5 × 5 × 12.5 cm^3 was used. Its freshly polished surface was clamped against a shallow stainless steel trough containing protein solution in D_2O. The incoming parallel neutron beam was directed into one end of the silicon block, reflected from the solid/D_2O solution interface, and exited from its other end. Measurements at three different incidence angles of 0.35°, 0.8°, and 1.8° were normalized against unity below the critical angle and combined. A flat background was subtracted from each measured reflectivity profile and its value was estimated by averaging the reflectivity measured at wave vectors above 0.3 Å^{-1}. Model fitting based on the optical matrix formula was used to obtain information about thickness (τ) and scattering length density (ρ) for adsorbed protein layer.[37] From the fitted ρ, the volume fraction of protein in the layer can be obtained.

The large ⟨111⟩ surface of the silicon block was polished following the same procedure as previously described.[24,25] The freshly polished surface was flashed by water, then ethanol, followed by 5% Decon solution. The entire block was then rinsed thoroughly with Elgastat ultrapure water (UHQ). The block was then soaked in acid peroxide solution (600 mL of 98% H_2SO_4 in 100 mL of 25% H_2O_2) for 2 min at 90 °C to optimize the surface hydrophilicity.[45−46] This set of surface treatments was found to produce very smooth surfaces with a very thin layer of oxide that was completely wettable by water.

The antibody used in this study was a mouse monoclonal anti-hCG (human chorionic gonadotropin) supplied by Unipath UK (clone no. 3468). It was directed against the β subunit of hCG. The molecular weight is 150 000 and the isoelectric point is around pH 6.0. HCG, purchased from Scipac Ltd (Kent, U.K.), was a human urine protein and was greater than 96% pure, lyophilized from 0.02 M NH_4HCO_3 (thus containing traces of buffer salts). It showed one band on SDS−PAGE corresponding to the hCG molecular weight. Crystal structures of the antibody, hCG, and the bound ternary complex between the two have been reported by Tegoni et al.[42] A recent low-resolution solution structure study using synchrotron radiation small-angle X-ray scattering coupled with the ab initio restoration of the macromolecular shape from the scattering data has revealed that IgG also adopted the distorted Y-type crystallographic model but has a swollen appearance reflecting the flexibility of the molecule in solution.[47] Previous Raman spectral studies of secondary structures by Fagnano and Fini[48] have also shown few changes in secondary structures of free antibodies and bound complexes in aqueous solution. The recent differential scanning calorimetry (DSC) and circular dichroism (CD) work by Vermeer and Norde[49] has shown the structural stability of IgG against pH and temperature as far as the current experimental pH range and temperature were concerned. In our study the solution pH was adjusted by varying the ratio of Na_2HPO_4, NaH_2PO_4, and H_3PO_4, with the total ionic strength kept fixed at 20 mM. All chemicals used in the present work were of AR grade and used as supplied. D_2O used contained over 99% D and was purchased from Sigma−Aldrich. Its surface tension was over 71 $mN \cdot m^{-1}$ at 298 K, indicating the absence of any surface-active impurity. All the glassware and troughs for the reflection measurements were cleaned with commercial detergent (Decon 90) followed by copious rinsing with UHQ water. All the experiments were performed at 298 K.

Antibody binding activity (AgBC) was measured by spectroscopic ellipsometry. The detailed experimental procedure has been described previously.[35] Briefly, the freshly cleaned bare silicon oxide surface was preadorbed with the antibody and the SE measurement was followed until 60 min from the start and the surface excess tended to plateau. The antibody solution was then replaced by buffer (10 min) and SE measurement continued to account for the rising effect. The buffer solution was then replaced by 1 mg/mL BSA to reduce nonspecific adsorption (20 min), and the SE was made to quantify BSA adsorption during the blocking stage. This was again followed by buffer rinsing (10 min) and SE measurement. The buffer was then replaced by 2 mg/L hCG solution at pH 7 with 20 mM PBS buffer for its binding measurement. Antibody adsorption by neutron reflection was measured under the same surface and solution conditions except that neutron reflection usually started some 30 min after the solution was in contact with the surface. Thus neutron reflection revealed the antibody's equilibrated layer structure and composition at different pH values.

Acknowledgment. We thank BBSRC for support under Grant 36/E19397, EPSRC for providing neutron beam time, and Unipath Ltd. for providing antibody and hCG. H.X. thanks China University of Petroleum and Unipath for financial support towards his research visit at University of Manchester.

References and Notes

(1) Herron, J. N.; Wang, H. K.; Janatová, V.; Durtschi, J. D.; Christensen, T. A.; Caldwell, K.; Chang, I. N.; Huang, S. J. In *Biopolymers at Interfaces*, 2nd ed.; Malmsten, M., Ed.; Marcel Dekker: New York, 2003; Chapt. 6.
(2) van Erp, R.; Linders, Y. E. M.; van Sommeren, A. P. G.; Gribnan, T. C. J. *J. Immumol. Methods* **1992**, *152*, 191.
(3) Butler, J. E.; Ni, L.; Brown, W. R.; Joshi, K. S.; Chang, J.; Rosenberg, B.; Voss, E. W. *Mol. Immunol* **1993**, *30*, 1165.
(4) Olson, W. C.; Spitznagel, T. M.; Yarmush, M. L. *Mol. Immunol*. **1989**, *26*, 129.
(5) Spitznagel, T. M.; Clark, D. S. *Nat. Biotechnol.* **1993**, *11*, 825.
(6) O'Shannessy, D. J.; Dobersen, M. J.; Quarles, R. H. *Immunol Lett.* **1984**, *8*, 273.
(7) Hoffman, W. L.; O'Shannessy, D. J. *J. Immunol. Methods* **1988**, *112*, 113.
(8) Chang, I. N.; Herron, J. N. *Langmuir* **1995**, *11*, 2083.
(9) Chang, I. N.; Lin, J. N.; Andrade, J. D.; Herron, J. N. *J. Colloid Interface Sci.* **1995**, *174*, 10.
(10) Buijs, J.; White, D. D.; Norde, W. *Colloids Surf. B* **1997**, *8*, 239.
(11) Chen, S.; Liu, L.; Zhou, J.; Jiang, S. *Langmuir* **2003**, *19*, 2859.
(12) Grabbe, E. S. *Langmuir* **1993**, *9*, 1574.
(13) Kamyshny, A.; Lagerge, S.; Partyka, S.; Relkin, P.; Magdassi, S. *Langmuir* **2001**, *17*, 8242.
(14) Perrin, A.; Lanet, V.; Theretz, A. *Langmuir* **1997**, *13*, 2557.
(15) Wink, T.; Zuilen, S. J. V.; Bult, A.; Bennekom, W. P. V. *Anal. Chem.* **1998**, *70*, 827.
(16) Malmsten, M. *J. Colloid Interface Sci.* **1998**, *207*, 186.
(17) Malmsten, M. *J. Colloid Interface Sci.* **1994**, *116*, 333.
(18) Harteveld, J.; Nieuwenhuizen, M.; Wils, E. *Biosens. Bioelectron*. **1997**, *12*, 661.
(19) Giacomelli, C. E.; Bremer, M. G. E. G.; Norde, W. *J. Colloid Interface Sci.* **1999**, *220*, 13.
(20) Fragneto, G.; Thomas, R. K.; Rennie, A. R.; Penfold, J. *Science* **1995**, *267*, 657.
(21) Liebmann-Vinson, A.; Lander, L. M.; Foster, M. D.; Brittain, W. J.; Vogler, E. A.; Majkrzak, C. F.; Satija, S. *Langmuir* **1996**, *12*, 2256.
(22) Petrash, S.; Liebmann-Vinson, A.; Foster, M. D.; Lander, L. M.; Brittain, W. J.; Majkrzak, C. F. *Biotechnol. Prog.* **1997**, *13*, 635.
(23) Su, T. J.; Lu, J. R.; Thomas, R. K.; Cui, Z. F.; Penfold, J. *J. Phys. Chem. B* **1998**, *102*, 8100.
(24) Su, T. J.; Lu, J. R.; Thomas, R. K.; Cui, Z. F.; Penfold, J. *Langmuir* **1998**, *14*, 438.
(25) Su, T. J.; Lu, J. R.; Thomas, R. K.; Cui, Z. F. *J. Phys. Chem. B* **1999**, *103*, 3727.
(26) Su, T. J.; Green, R. J.; Wang, Y.; Murphy, E. F.; Lu, J. R.; Ivkov, R.; Satija, S. K. *Langmuir* **2000**, *16*, 4999.
(27) Su, T. J.; Lu, J. R.; Thomas, R. K.; Cui, Z. F.; Penfold, J. *J. Colloid Interface Sci.* **1998**, *203*, 419.
(28) Petrash, S.; Cregger, T.; Zhao, B.; Pokidysheva, E.; Foster, M. D.; Brittain, W. J.; Sevastianov, V.; Majkrzak, C. F. *Langmuir* **2001**, *17*, 7465.
(29) Tiberg, F.; Nylander, T.; Su, T. J.; Lu, J. R.; Thomas, R. K. *Biomacromolecules* **2001**, *2*, 844.
(30) Choi, E. J.; Foster, M. D.; Daly, S.; Tilton, R.; Przybycien, T.; Majkrzak, C. F.; Witte, P.; Menzel, H. *Langmuir* **2003**, *19*, 5464.
(31) Forciniti, D.; Hamilton, W. A. *J. Colloid Interface Sci.* **2005**, *285*, 458.
(32) Cooper, A.; Kennedy, M. W.; Fleming, R. I.; Wilson, E. H.; Videler, H.; Wokosin, D. L.; Su, T. S.; Green, R. J.; Lu, J. R. *Biophys. J.* **2005**, *88*, 2114.
(33) Xu, H; Zhao, X. B.; Grant, G.; Lu, J. R.; Williams, D. E; Penfold, J. *Langmuir* **2006**, *22*, 6313.
(34) Buijs, J.; van den Berg, P. A. W.; Lichtenbelt, J. W. T.; Norde, W; Lyklema, J. *J. Colloid Interface Sci.* **1996**, *178*, 594.
(35) Xu, H.; Lu, J. R.; Williams, D. E. *J. Phys. Chem. B* **2006**, *110*, 1907−1914.
(36) Iler, R. K. *The Chemistry of Silica*; Wiley: New York, 1979.
(37) Lu, J. R.; Lee, E. M.; Thomas, R. K. *Acta Crystallogr.* **1996**, *A52*, 11−41.
(38) Lu, J. R.; Su, T. J.; Thomas, R. K.; Penfold, J.; Richards, R. W. *Polymer* **1996**, *37*, 109.
(39) Silverton, E. W.; Navia, M. A.; Davies, D. R. *Proc. Natl. Acad. Sci. U.S.A.* **1977**, *74*, 5140.
(40) Deisenhofer, J. *Biochemistry* **1981**, *20*, 2361.
(41) Marquart, M.; Deisenhofer, J.; Huber, R.; Palm, J. *J. Mol. Biol*. **1980**, *141*, 369.
(42) Tegoni, M.; Spinelli, S.; Verhoeyen, M.; Davis, P.; Cambillau, C. *J. Mol. Biol*. **1999**, *289*, 1375.
(43) Shimojo, M.; Sakakibara, R.; Ishiguro, M. *J. Biochem. (Tokyo)* **1993**, *114*, 83−87.
(44) Fellegvari, I.; Valko, K.; Varadi, G.; Bauer, P.; Kramer, M. *Chromatographia* **1989**, *27*, 601−604.
(45) Vig, J. R. *Vac. Sci. Technol*. **1985**, *A3*, 1027.
(46) Cullen, D. C.; Lowe, C. R. *J. Colloid Interface Sci.* **1994**, *166*, 102.
(47) Volkov, V. V.; Lapuk, V. A.; Kayushina, R. L.; Shtykova, E. V.; Varlamova, E. Y.; Malfois, M.; Svergun, D. I. *J. Appl. Crystallogr.* **2003**, *36*, 503−508.
(48) Fagnano, C.; Fini, G. *J. Mol. Struct.* **1993**, *294*, 111−114.
(49) Vermeer, A. W. P.; Norde, W. *Biophys. J.* **2000**, *78*, 394−404.

BM070297U